Design and Synthesis of inhibitors of tumor necrosis factor-alpha (TNF) activity of patients with Rheumatoid arthritis (RA)

1 author:

Faiq Isho Gorial

University of Baghdad

249 PUBLICATIONS   **769** CITATIONS

Design and Synthesis of inhibitors of tumor necrosis factor-alpha (TNFα) activity of patients with Rheumatoid arthritis (RA)

Mohammed Yaseen Al-Samaree[1]*, Mohammed Ibraheem Nader[2], Faiq I. Gorial[3], Jalal A. Al-Tuama[4], Moamel Hadi Yaseen5

[1,2]Institute of Genetic Engineering and Biotechnology-Baghdad University/Iraq
[3]Rheumatology Unit, Department of Medicine, College of Medicine, University of Baghdad, Baghdad, Iraq.
[4]Veterinary directorate--Ministry of Agriculture/Iraq
[5]College of Science, Department of Chemistry, University of Baghdad/Iraq
Email: mohammedsmary251@gmail.com

Abstract

Tumor necrosis factor-alpha (TNF-α) is a pro-inflammatory cytokine. It acts as a biological regulator of immune function, but its dysregulation is associated with a number of diseases, especially autoimmune diseases. The strategy of inhibiting TNF-α is an excellent treatment option for autoimmune diseases. This study uses computational methods to design potential inhibitors against TNF-α. The Lipinski rule, molecular docking, and ADMET studies identified the results as active agents. They were evaluated to gain insight into the potential binding interaction with the target protein. Based on that, three compounds (MY1, MY2 and MY3) were selected for synthesizing and studying their activity in the laboratory. The molecules were examined for their purity and identity and confirmed by their melting points, FT-IR and H1NMR-spectra. The laboratory evaluation results showed the three compounds classified within the medium toxicity compounds, on the other hand, the values of Kd were (0.129 µM, 10.19 µM, 0.389 µM) and IC50 were (4.34 nM, 4.50 nM and 4.60 nM,) respectively. ΔG has also calculated the values (-9.44 Kcal/ mole), (-6.8 Kcal/ mole) and (8.35 Kcal/ mole). The bonding efficiency scores showed (LE ≤ 0.3), which indicates that all compounds capable of inhibiting TNF-alpha significantly.

1. Introduction

Rheumatoid arthritis (RA) is one autoimmune disease characterized by chronic inflammation of the joints. it is an unknown etiology, widespread in almost all human populations , affects 0.5 to 1% of the world's population [1]. usually affects women at a higher rate than men , and generally occurs later in life [2]. It mainly affects joints' synovial membranes, leading to cartilage and bone damage. This disease can damage different body systems, such as the skin, eyes, lungs, heart, and blood vessels. In addition to chronic pain, fatigue, and possible disability, RA patients also exhibit increased morbidity and mortality, primarily from cardiovascular disease [1].Tumor Necrosis Factor-alpha (TNFα) has critical cell functions including cell proliferation, survival, differentiation, and apoptosis are regulated by TNFα signals through two transmembrane receptors, TNFR1 and TNFR2 [3]. TNFα also is one of the pro-inflammatory cytokines which play a major role in the progress of different autoimmunity diseases such as rheumatoid arthritis (RA). Many experimental studies have demonstrated that when TNFα increased that plays a significant role in local joint damage and systemic bone loss, as it increases osteoclast (OC) mediated bone resorption [4]. Therefore, this study aims to design and evaluate compounds that can function as tumor necrosis factor-alpha (TNFα)

inhibitors.

2. Materials and Method

Computational based analysis

The research referred that the complex crystal structure of TNF-α with SPD304 ligand (PubChem CID: 5327044) and with UCB-9260 ligand (PubChem CID: 72700327) showed effective inhibition of TNF-alpha [5] therefore used in the study TNF-α dimer complex structure with a small molecule inhibitor as references to determine pocket on the surface of TNF-alpha. From PDB (Protein Data Bank) obtained a complex of TNF-alpha and ligand (PDB ID: 2AZ5) and crystal structures of TNF-α (PDB ID: 6OP0). The active amino acid sites of the complex structure of TNF-α were predicted using structure comparison and site finder algorithms.

Molecules Design

Select different materials that have an active group that can interact with a side chain with a greater frequency of amino acids in the active site.
Molecular docking studies are used to examine ligands designed or compounds obtained from pharmacophore-based screening. All hits are docked at the active site of the target protein. Used the MOE docking algorithm to bind SPD304 to the active site. The most effective hit is selected based on the S

score value of the PSD34 inhibitor and root mean square deviation (RMSD). The S value is a score that measures the affinity between the ligand and the receptor and is calculated by the default score construction function in the MOE.

ADME profile of Molecules

The compounds were further evaluated by the ADMET (metabolism, distribution, excretion, absorption, and toxic properties by using the ADMET SAR server. The ADMET algorithm was used to predict the properties of the designed compounds and drug candidates.

Chemical Studies

The synthesis of the designed compounds was achieved by following a general method below.
the carboxylic acid was dissolved in ten volumes of dry solvent treated with one equivalent of dry pyridine, and then exactly one equivalent of purified thinly chloride was added, drop-wise with stirring. Pyridine hydrochloride separated, and the mixture was left at 15°C -20°C for an hour. The amine to be coupled with the acid chloride was mixed with one equivalent of pyridine, and added drop-wise with stirring; then the amide was recovered and purified by the usual methods [6]. All chemicals were of the highest purity. Melting point apparatus of Gallen-Kamp MFB 600 was used to measure the melting point of synthesized compounds. The infrared spectra of synthesized compounds were carried out by using Infrared spectra in the range (4000-600) cm⁻¹ and were recorded without a KBr disc on FTIR 8300 Shimadzu spectrophotometer. This measurement was carried out in the Chemistry Department, College of science Baghdad University, H1NMR-spectra in (ppm) –unit was obtained in DMSO solution using (Bruker, Ultra Shield 300 MHz Switzerland), (Iran).

MTT assay

This assay was performed and IC50 sample values were calculated using the dose-inhibition curve. In this procedure or examination, the cytotoxicity effect of all compounds was determined. On the line of natural rat cells grown and prepared in Biotechnology Research Center/Al-Nahrain University (Iraq). The method: Normal cells of the rat were prepared (1 × 104 to 1 ×106 cells ml). The cells were then placed in a plate containing 96 holes with a flat base volume of 100 μl/well. The dishes were covered with sterile Para film and then they were stirred. It was incubated in a 5% incubator. CO2 at 37°C for 24 hours and after incubation the RPMI media was removed. The prepared concentrations of the ligands were added to the culture medium. Record absorbance at 570 nm. Statistical analysis of optical density readings Calculate IC50 according to the following equation:

Viability (%) = (optical density of sample / Optical density of control) 100%

Thermos shift assay

TNF-alpha used in this assay was imported from Cusabio company with a purity of >90%. Prepare protein assay stock in HEPES buffer (0.01 M HEPES stock solution at pH 7.4). Thermal Shift Assay (TSA) test run for the determination of the optimal amount of protein. Prepare a dilution series of your protein sample in buffer /DMSO ranging from 0.03 to 0.5 μM final concentration in a total volume of 25 μl. Export the file into Microsoft Excel analyses [7]. Fit fluorescence intensity curve to a Boltzmann sigmoidal curve using TSA_CRAFT service to obtain the melting temperature (Tm) of the protein Calculate: ΔTm = Tm ligand - Tm buffer/DMSO. A positive Tm indicates that the ligand stabilizes the protein from denaturation. Data Analysis to Determine the Dissociation (kd) Constant under Thermal Denaturation. Created a table in Excel of the ligand concentrations and the melting temperature. Analyze the data using the following equation.

$$Y= \text{Bottom} + ((\text{Top-Bottom}) (1-((P- K_d -X+ \sqrt{((P+X+K_d)^2-(4PX))}) /(2P))))$$

Where P: protein concentration. Kd: dissociation constant (has the same unit as P). T: melting temperature at high inhibitor concentration; B: melting temperatures of no inhibitor concentration.

Calculate ΔG and LE

recommended to assess binding affinity in relation to the number of heavy atoms in a molecule and The calculation of the binding energy(ΔG) of the ligand and ligand efficiency (LE): Calculate Free energy of ligand binding: $\Delta G = -RT.\ln K_d$. Calculate Binding energy per atom (ligand efficiency (LE)): $LE = \Delta G/N_{\text{non-hydrogen atoms}}$

inhibitory concentration (IC50).

Serum Allow serum to clot for 10-20 minutes at room temperature. Centrifuge at 2000-3000 RPM for 20 minutes. Collect the supernatant without sediment. Using the manufacturer's ELISA analysis method with changing steps related to the experiment, the susceptibility of ligands to protein inhibition by the sample addition step. Prepare all reagents, standard solutions and samples as instructed. Bring all reagents to room temperature before use. The assay is performed at room temperature. IC50s values were determined by fitting a dose-response curve (four parameters) to inhibition (%) to the data, using GraphPad Prism software [8].

3. Results and Discussion

The active amino acid sites of the complex structure of TNF-α were predicted using structure comparison and site finder algorithms. the matching tool in the structure comparison algorithm in the chimaera program showed the overlap in the binding site for both the complex structure of the TNF-α dimer with SPD304 and with UCB-9260. Also used the site finder algorithm to produce a catalytic site of TNF-α. The pocket was predicted size (95), and hydrogen (49). side chain (60), site amino acids (Leu57, Tyr59, Tyr119, Gly121, Val123, Ile155, Leu157) of Chain-A, (Leu57, Ile58, Tyr59, Tyr119, Gly121, Gly122,

Leu157) of Chain-B, (Leu57, Tyr59, Ser60, Gln61, Tyr119, Leu120, Gly121, Tyr151, Ile155) of Chain-C. According to the active sites, a compound suggests with functional groups that can interact with the side chain of the active site and bind with the lowest binding energy. The most effective hit is selected based on the S score value of the PSD34 inhibitor and root mean square deviation (RMSD). The S value is a score that measures the affinity between the ligand and the receptor and is calculated by the default score construction function in the MOE [9]. The RMSD is used to compare the docking confirmation with the docking reference configuration. Depend on lower S and RMSD values when selecting [10].

Three molecules were selected from the designed compounds as a result of ADMET profiling analysis, which are shown in Figure (1) and Table (1). The molecules MY1, MY2 and MY3 contains NH-donor functional groups in addition to the acceptor functional groups (carbonyl groups) and the sulfur group in MY2 as a donor, as well as the hydrophobic and aromatic groups in the selected compounds.
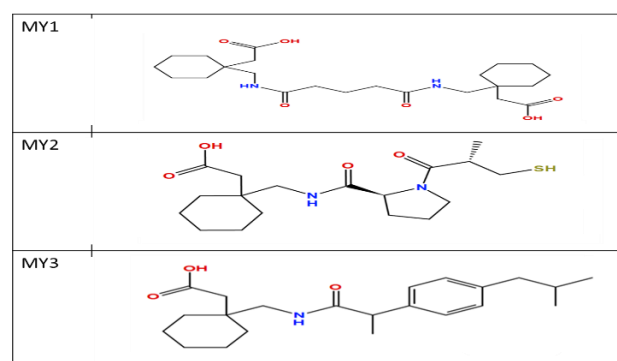

Figure (1): Three designed molecules (red colored groups represent H-acceptors while blue groups represent H-donors and yellow color represents Sulfur group).

Table (1): Symbols, Molecular formula and IUPAC nomenclature of Designed Molecules		
Symbols	IUPAC nomenclature	Molecular formula
MY1	[1,1'- ((5,5'-oxopentanamido) methyl)) cyclohexyl] acetic acid	$C_{33}H_{38}N_2O_6$
MY2	[1(2S)-1-[(2S)-2-methyl-3-sulfanylpropanoyl] pyrrolidine-2-carboxamide) cyclohexyl]acetic acid	$C_{26}H_{31}N_2O_4S$
MY3	(1-([2[-(4-methyl propyl) phenyl] propanamido] methyl) cyclohexyl) acetic acid	$C_{29}H_{40}NO_3$

The S score ≥ -7.5 and RMSD ≥2 were selected for screening small molecules. The design compounds showed a good interaction compared to the reference ligand showed in Table (2).

Table (2): The docking score of compounds and interaction types.					
Compounds	S-Score	RMSD	Number of interaction types		
			Hydrophobic	Hydrogen	Other
MY1	-9.13	-1.69	10	5	3
MY2	-8.33	-1.82	8	4	0
MY3	-8.25	-1.33	11	4	0
SPD304 (Reference)	-8.4	-1.79	9	4	0

Table (2) showed the interactions between ligand and protein were detected by the web service The protein-ligand interaction profiler (PLIP) for fully automated detection and visualization of relevant non-covalent protein-ligand contacts in 3D structures [11] . All compounds showed binding with the side chain of amino acid in the active site of the target protein with many hydrogen bonds, hydrophobic, other which include in MY1 salt bridge (bonds between oppositely charged residues) . The compounds (MY1) shouted affinity (S score) highest than reference ligand and (MY2, MY3) showed good affinity compared to the reference ligand. molecular docking of compounds was displayed in Figure (2).
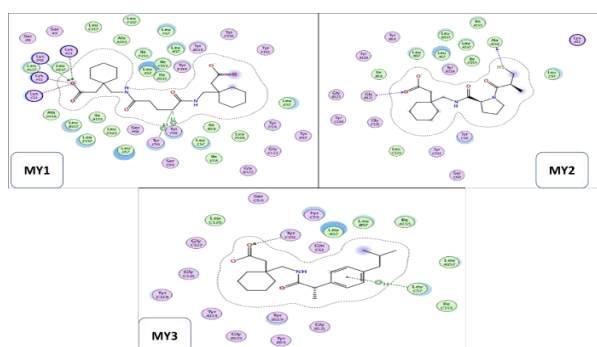

Figure (2): Molecular Docking of Molecule (MY1, MY2 and MY3)

To distinguish the drug-like and non-drug-like properties compounds were evaluated based on the Lipinski rule (molecular mass: ≤500 Daltons, hydrogen bond donor: <5, hydrogen bond acceptor: <10 molars refractive index: 40-130, and partition coefficient (logP): ≤5) [12]. Table (3) showed that all designed molecules were within the molecular weight 'MW' range of six descriptors (from 359.5 to 451.48 g/mole). Meanwhile logarithm of lipophilicity 'log P' (octane-water partition coefficient) was (0.58 to 2.23) within the normal range of known drugs.

All designed molecules are suitable and not too polar to dissolve in the bloodstream and eliminated so easily and not too lipophilic to eliminate from the bloodstream by the liver which is consistent with what the researchers pointed out [12] . The compounds were further evaluated by the ADMET (metabolism, distribution, excretion, absorption, and toxic properties using the ADMET SAR server.

The compounds significantly accepted these parameters of the ADMET table (4). Only those ligands were considered to be the potential drug candidates that accomplished all the ADMET models successfully.
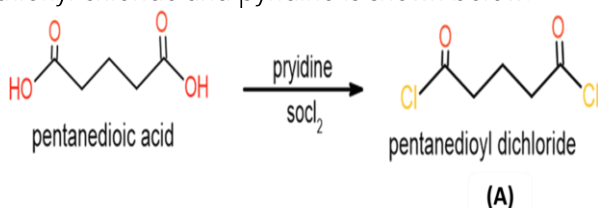
Table (3): Drug likeness scores of selected compounds.				
Five roles	MY1	MY2	MY3	Range
MW	436.5	370	359.5	< 500
HBD	2	2	2	< 5
HBA	6	4	3	< 10
LogP	0.57	2.08	4.53	< 5
tPSA	138.46	125.5	66.40	< 140

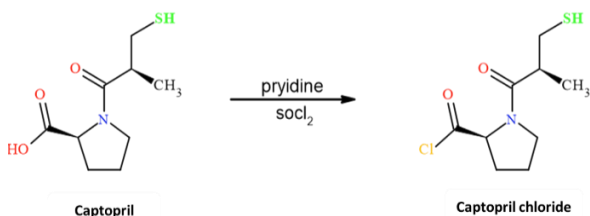| Table (4): ADMET Predictor Profile and Classification.					
Molecules					
Absorption	MY1	MY2	MY3		
Caco2-Permeability	-	-	+		
Blood-Brain Barrier	+	-	+		
Human Intestinal Absorption	+	+	+		
P-glycoprotein Inhibitor	NI	NI	I		
Metabolism	MY1	MY2	MY3		
CYP450 1A2 Inhibitor	NI	NI	NI		
CYP450 2C9 Inhibitor	NI	NI	NI		
CYP450 2D6 Inhibitor	NI	NI	NI		
CYP450 2C19 Inhibitor	NI	NI	NI		
CYP450 3A4 Inhibitor	NI	NI	I		
Toxicity	MY1	MY2	MY3		
AMES toxic	NO	NO	NO		
Carcinogenic	NO	NO	NO		
Toxicity Class	4	5	4		

Several compounds that have shown the ability to interact with protein and have low toxicity are designed (in silico). Three of these compounds were selected and synthesized by the following methods The synthesis of the MY1 compound from the reaction of pentanedioic acid with the equivalent of thionyl chloride and pyridine is shown below.
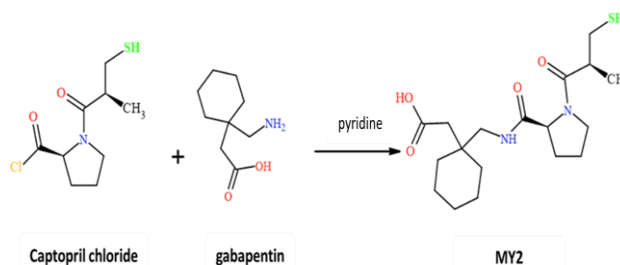

The (A) compound to the new flask to get rid of Side products . Then an equivalent of gabapentin was added in the reaction to form the MY1 compound in the presence of pyridine shown below.
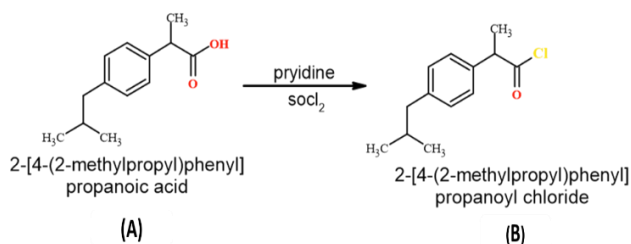

the MY2 was synthesized by reacting Captopril with the equivalent of thionyl chloride and pyridine as shown below.
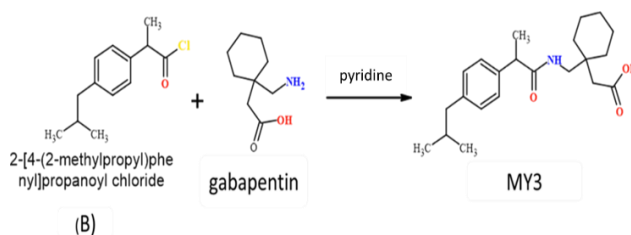

thionyl chloride was added, dropwise with stirring. Then, in the presence of pyridine, an equivalent of gabapentin was added to the process to produce the MY2 compound as shown below.

the MY3 was synthesized by reacting compound (A) with the equivalent of thionyl chloride and pyridine to produce compounded B shown below.

After that, the mixture was left at 15-20 °C for 1 hour. Then, in the presence of pyridine, an equivalent of gabapentin was added to compound (B) to produce the MY3.

All mixture was left for an hour at room temperature. The compounds were separated by liquid-liquid methods. The solvent was removed by a rotary evaporator. The physical parameters of the compounds were MY1 light brown solid with has melting point (82°C -84°C), MY2 was yellowish-brown solid with a melting point (88 °C-91 °C), MY3 was a pale-yellow solid with (54 °C -56°C).

spectral data. FTIR spectrum (Figures (4); (5) and (6)) showed the intense bands at 3258 cm-1 and 3394 cm-1 for amide groups, as well as intense bands at 1581 cm-1 and 1619 cm-1 for carboxylic acid carbonyl and bands at 1683 cm-1 and 1713 cm-1 for amide group carbonyl, suggest that the interaction of gabapentin and carboxylic chloride is successful, which confirms the formation of compounds (MY1, MY2 and MY3).

the H-NMR analysis was used to identify the synthesized compounds. the spectra were recorded using DMSO solvent the values of the characteristics of the chemical shift were Interpreted by using ACD/ lab software which was designed to interpret the NMR result according to the literature curve of analogue compounds and references chemicals. the result report summarized in table (5).

Table (5): H-NMR (δ ppm, DMSO) of Compounds
Comp. No.	H-NMR
MY1	1.40 (br. s., 23 H), 1.96 (s, 4 H), 2.97 (s, 4 H), 7.46 (br. s., 2 H
MY2	1.42 (br s, 22 H) 1.98 (br s, 3 H) 2.98 (br s, 3 H) 7.45 (br s, 1 H)
MY3	m 0.86 (br d, J=6.58 Hz, 5 H) 1.35 (br d, J=7.13 Hz, 6 H) 1.42 (br s, 12 H) 1.98 (s, 2 H) 2.42 (br d, J=7.13 Hz, 2 H) 2.99 (s, 2 H) 7.10 (br d, J=8.23 Hz, 2 H) 7.19 (br d, J=8.23 Hz, 2 H)
	s = singlet, d = doublet, br = broad signal, J= coupling constant.

Cytotoxicity assays in vitro bioassay methods are used to predict the toxicity of substances to various tissues. In vitro cytotoxicity testing provides a crucial method for safety assessment and screening compounds [13]. The cytotoxic effect of the synthesis compounds was determined by the MTT test performed using a normal rat cell line where IC50 (or lethal dose, 50%) values were determined by fitting a dose-response curve (four parameters: the bottom and top plateaus of the curve, the IC50, and the slope factor) to inhibition (%) to the data, using GraphPad Prism Software figure (3). The (IC50) results for MY1, MY2, MY3 were 1351 µg/ml, 941.3 µg/ml and 375.7 µg/ml, respectively. The compounds classification is based on IC50 to (10–100 µg/m strong cytotoxicity) and (100–500 µg/mL moderate cytotoxicity) [14]. thus the compound MY3 is considered moderately toxic, while the two MY1 and MY2 compounds have low toxicity.
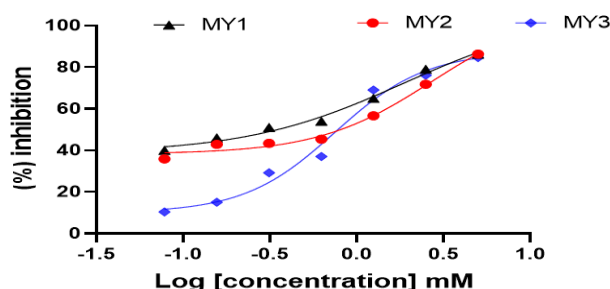

Figure (3): Curve Fitting percentage inhibition versus log of ligand concentration to determine IC50 synthesis compounds (R2 ≥ 0.98).

The results showed that the melting temperature Tm increased with the increase in the concentration of the inhibitor, which indicates the binding of the inhibitor to the protein at the site where the stability of the protein increases. Indicating that the inhibitors positively correlate with TNF-alpha. Figures (4), (5) and (6). The values of ΔTm are significant. where any small molecule yielding ΔTm > 2.0 °C was indicated as a hit potential [15]. The increase in ΔTm was also observed with increasing bonding concentration, this means the stability of the TNF-alpha increases with the increasing concentration of the inhibitor,

indicating the affinity of the compounds to the protein the researchers pointed to that ΔTm is for the higher affinity inhibitor and decreased when the affinity decreases [16].

Kd is the dissociation constant and is the ligand concentration, which correlates with half of the binding sites on the protein in a balanced system and is considered an indicator of selectivity [17] . Kd values were as follows 0.129 µM, 10.19 µM, 0.389 µM . The best values for kd are in MY1 being the lowest values compared to the other compounds, while the highest values are in the compound MY2. when higher the Kd value, the lower the correlation and the lower the interactions, the opposite occurs when the Kd value is low. the kd value of all ligands is acceptable, they are within the range of moderate affinity. In biochemistry or pharmacology, the binding affinity range of Protein interactions is considered to have high affinity if Kd is less than 10 nM (for antibody-antigen complex), medium affinity in the 10 nm-100 µM range, and low affinity if Kd is above 100 µM [18]. The dissociation constant represents the partial saturation as a function of the free bonding concentration. Once the Kd of a particular protein-ligand composition has been determined, it is possible to predict partial saturation at any ligand concentration [19].
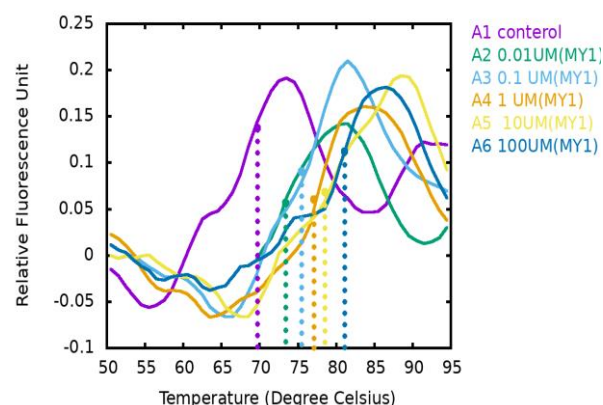

Figure (4): Thermal shift curves of unfolding transition of TNF-alpha in the presence of 100 µM, 10 µM, 1 µM, 0.1 µM 0.01 µM, and 0 µM of MY1. Data fit Boltzmann equation gave midpoint Tm of 81.13℃, 78.52℃, 77.07.5℃, respectively, (R2 ≥ 0.9).
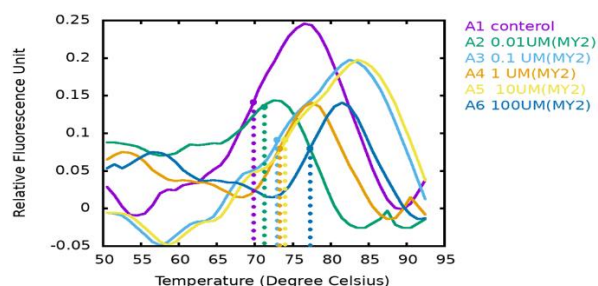
Figure (5): Thermal shift curves of unfolding transition of 0.5 µM TNF-alpha in the presence of 100 µM, 10 µM, 1 µM, 0.1 µM 0.01 µM, and 0 µM of MY2. Data fit Boltzmann equation gave midpoint Tm of 81.13°C, 78.52°C, 77.07.5°C, 75.48°C, 73.38°C and 69.69°C, respectively, ($R2 \geq 0.9$).
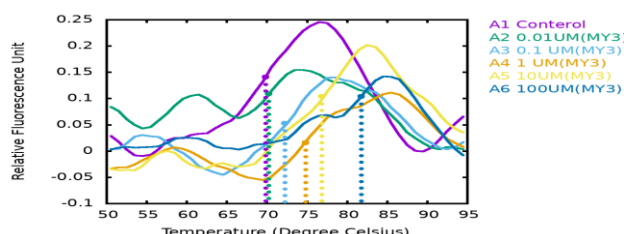

Figure (6): Thermal shift curves of unfolding transition of 0.5 µM TNF-alpha in the presence of 100 µM, 10 µM, 1 µM, 0.1 µM 0.01 µM, and 0 µM of MY3. Data fit Boltzmann equation gave midpoint Tm of 81.80°C, 76.81°C, 74.81°C, 72.26°C, 70.26°C and 69.83°C, respectively, ($R2 \geq 0.9$).

One of the methods for evaluating drug-like compounds is by calculating ligand efficiency (LE), where ligand efficiency refers to the ability of a ligand to produce a biological response upon binding to the target receptor and the quantitative quantity of this response, the smaller ligands bind more efficiently when comparing the binding affinity per heavy atom [20]. On the other hand, the spontaneity of the reaction is determined based on the Gibbs free energy (ΔG) value where Negative values indicate that the reaction occurs spontaneously [21] . The value of ΔG was calculated based on the kd values, by converting the Kd into the free energy of binding at 300K, LE is useful in ligand assessment and can be calculated by dividing ΔG by the number of heavy atoms (non-hydrogen atoms) [22]. as shown in table (6).

Table (6): The value of (ΔG) and the value of (LE)			
Inhibitor Nam	(ΔG) Kcal/ mole	Heavy atoms	(LE) Kcal/ mole/ HA
MY1	-9.44	41	0.230
MY2	-6.84	33	0.207
MY3	-8.35	33	0.253

The results of (LE) showed a ligand capable of significantly inhibiting TNF-alpha. Evaluated based on ligand efficiency scores (LE ≤ 0.3) [23]. hat compounds have high 'ligand efficiency' (binding affinity per heavy atom) and so are highly suitable for optimization into clinical candidates with good drug-like properties [24].

IC50 is the most widely used and most informative measure of drug effectiveness. Refers to the amount of drug required to inhibit half of the biological activity [25]. A patient serum sample was used in this analysis to measure the effect of the compounds on TNF-alpha, and dilutions of the ligand added to the serum. The serum - ligand was left for 30 min at 37 °C to allow the interaction to occur. The (IC50) results for MY1, MY2 and MY3, were 4.34 nM, 4.50 nM and 4.60 nM, respectively. The curve (Figure (7) showed that all compounds were highly effective in inhibiting TNF-alpha, as the percentage of protein inhibition increased when the concentration of the compounds increased, this occurs as a result of the binding of the inhibitors at a position that prevents the protein from binding with an antibody coating in the Elisa plate.
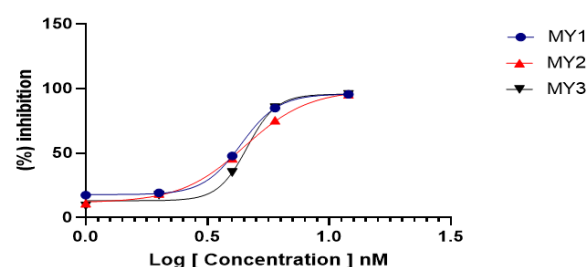

Figure (7): Curve Fitting percentage inhibition versus log of ligand concentration to determine IC50 of MY1 ($R2 \geq 0.9$).

4. Conclusions

In this study, TNF-α inhibiting compounds were designed by computer methods, these compounds were evaluated in vitro. Experimental verification indicated that the three compounds classified within the medium toxicity also showed a significant ability to bind with TNF-α. It also showed the ability to inhibit TNF-α. The compounds can regulate the levels or activity of TNF-α and can be an economical alternative to antibody therapies. The inhibitors identified could serve as a stepping stone in developing new drugs.

5. Acknowledgment

Authors' contributions

All authors contributed to data analysis, drafting, and revising of the paper and agreed to be responsible for all the aspects of this work.

References

[1] E. Gómez-Bañuelos, A. Mukherjee, E. Darrah, F.J.J.o.c.m. Andrade, Rheumatoid arthritis-associated mechanisms of Porphyromonas gingivalis and Aggregatibacter actinomycetemcomitans, 8 (2019) 1309.

[2] E.G. Favalli, M. Biggioggero, C. Crotti, A. Becciolini, M.G. Raimondo, P.L.J.C.r.i.a. Meroni, immunology, Sex and management of rheumatoid arthritis, 56 (2019) 333-345.

[3] S. Naserian, M.E. Abdelgawad, M. Afshar Bakshloo, G. Ha, N. Arouche, J.L. Cohen, B.L. Salomon, G.J.C.c. Uzan, signaling, The TNF/TNFR2 signaling pathway is a key regulatory factor in endothelial progenitor cell immunosuppressive effect, 18 (2020) 1-14.

[4] M. Rajabinejad, F. Salari, A. Gorgin Karaji, A.J.A.c. Rezaiemanesh, nanomedicine,, biotechnology, The role of myeloid-derived suppressor cells in the pathogenesis of rheumatoid arthritis; anti-or pro-inflammatory cells?, 47 (2019) 4149-4158.

[5] B. Shivaleela, S. Srushti, S. Shreedevi, R.J.F.J.o.P.S. Babu, Thalidomide-based inhibitor for TNF-α: designing and Insilico evaluation, 8 (2022) 1-10.

[6] J. Human, J.A.J.N. Mills, Action of thionyl chloride on carboxylic acids in presence of pyridine, 158 (1946) 877-877.

[7] J.M. Dziekan, G. Wirjanata, L. Dai, K.D. Go, H. Yu, Y.T. Lim, L. Chen, L.C. Wang, B. Puspita, N.J.N.P. Prabhu, Cellular thermal shift assay for the identification of drug–target interactions in the plasmodium falciparum proteome, 15 (2020) 1881-1921.

[8] J.D. Baker, R.L. Uhrich, G.C. Kraemer, J.E. Love, B.C.J.P.o. Kraemer, A drug repurposing screen identifies hepatitis C antivirals as inhibitors of the SARS-CoV2 main protease, 16 (2021) e0245962.

[9] Z. Haider, M.M. Subhani, M.A. Farooq, M. Ishaq, M. Khalid, R.S.A. Khan, A.K.J.P. Niazi, In Silico discovery of novel inhibitors against main protease (Mpro) of SARS-CoV-2 using pharmacophore and molecular docking based virtual screening from ZINC database, (2020).

[10] S. Quazi, J. Malik, K.S. Suman, A.M. Capuzzo, Z.J.B. Haider, Discovery of potential drug-like compounds against Viral protein (VP40) of Marburg Virus using pharmacophoric based virtual screening from ZINC database, (2021).

[11] F. Bonnardel, J. Mariethoz, S. Salentin, X. Robin, M. Schroeder, S. Perez, F. Lisacek, A.J.N.a.r. Imberty, UniLectin3D, a database of carbohydrate binding proteins with curated information on 3D structures and interacting ligands, 47 (2019) D1236-D1244.

[12] Z. Yan, G.W. Caldwell, Cytochrome P450: In Vitro Methods and Protocols, Cytochrome P450, Springer2021, pp. 1-25.

[13] S. Lungu-Mitea, J.J.A.o.t. Lundqvist, Potentials and pitfalls of transient in vitro reporter bioassays: interference by vector geometry and cytotoxicity in recombinant zebrafish cell lines, 94 (2020) 2769-2784.

[14] G. Indrayanto, G.S. Putra, F.J.P.o.D.S. Suhud, Excipients, R. Methodology, Validation of in-vitro bioassay methods: Application in herbal drug research, 46 (2021) 273-307.

[15] S. Javaid, H. Zafar, M.I.J.B.C. Choudhary, Drugs repurposing: An approach to identify new hits against anticancer drug target TFIIH subunit p8, 124 (2022) 105755.

[16] V. Gapsys, L. Pérez-Benito, M. Aldeghi, D. Seeliger, H. Van Vlijmen, G. Tresadern, B.L.J.C.S. de Groot, Large scale relative protein ligand binding affinities using non-equilibrium alchemy, 11 (2020) 1140-1152.

[17] O.W. Mak, R. Chand, J. Reynisson, I.K.J.I.j.o.m.s. Leung, Identification of isoform-selective ligands for the middle domain of heat shock protein 90 (Hsp90), 20 (2019) 5333.

[18] M.-L. Malarte, A. Nordberg, L.J.E.J.o.N.M. Lemoine, M. Imaging, Characterization of MK6240, a tau PET tracer, in autopsy brain tissue from Alzheimer's disease cases, 48 (2021) 1093-1102.

[19] H.T. Rube, C. Rastogi, S. Feng, J.F. Kribelbauer, A. Li, B. Becerra, L.A. Melo, B.V. Do, X. Li, H.H.J.N.B. Adam, Prediction of protein–ligand binding affinity from sequencing data with interpretable machine learning, (2022) 1-8.

[20] K. Karl, M.D. Paul, E.B. Pasquale, K.J.J.o.B.C. Hristova, Ligand bias in receptor tyrosine kinase signaling, 295 (2020) 18494-18507.

[21] B.J.S.A.P.A.M. Tüzün, B. Spectroscopy, Investigation of pyrazoly derivatives schiff base ligands and their metal complexes used as anti-cancer drug, 227 (2020) 117663.

[22] P. Kirsch, A.M. Hartman, A.K. Hirsch, M.J.M. Empting, Concepts and core principles of fragment-based drug design, 24 (2019) 4309.

[23] P.W.J.J.o.C. Kenny, The nature of ligand efficiency, 11 (2019) 1-18.

[24] S. Chamakuri, S. Lu, M.N. Ucisik, K.M. Bohren, Y.-C. Chen, H.-C. Du, J.C. Faver, R. Jimmidi, F. Li, J.-Y.J.P.o.t.N.A.o.S. Li, DNA-encoded chemistry technology yields expedient access to SARS-CoV-2 Mpro inhibitors, 118 (2021) e2111172118.

[25] M. Plaze, D. Attali, M. Prot, A.-C. Petit, M. Blatzer, F. Vinckier, L. Levillayer, J. Chiaravalli, F. Perin-Dureau, A.J.I.j.o.a.a. Cachia, Inhibition of the replication of SARS-CoV-2 in human cells by the FDA-approved drug chlorpromazine, 57 (2021) 106274.